ARTICLES

The Photochemical Rearrangement Pathways of Imidazoles: A Theoretical Study
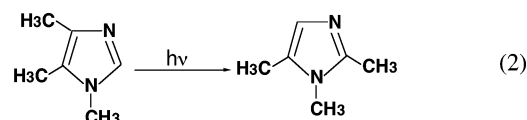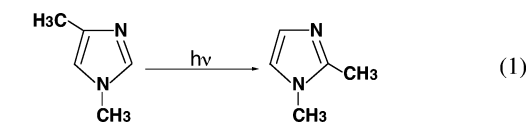
Ming-Der Su[†]

Department of Applied Chemistry, National Chiayi University, Chiayi 60004, Taiwan

Received: August 16, 2006; In Final Form: January 3, 2007

The mechanisms of the two reaction pathways for the photochemical transformations of methyl substituted imidazoles (i.e., 1,4-dimethyl-imidazole and 1,4,5-trimethyl-imidazole) in their first excited state ($^1\pi \rightarrow {}^1\pi^*$) have been determined using the CASSCF (10-electron/8-orbital active space) and MP2-CAS methods with the 6-311(d) basis set. These two reaction pathways are denoted as the conical intersection path (path 1) and the internal cyclization−isomerization path (path 2). Our model investigations suggest that conical intersections play a crucial role in the photorearrangements of imidazoles. Additionally, the present theoretical findings suggest that photoisomerizations of imidazoles via path 1 should adopt the reaction path as follows: imidazole → Franck−Condon region → conical intersection → photoproduct. Moreover, we have examined the alternative mechanism, the internal cyclization−isomerization path (path 2), which consists of a sequence of small geometric rearrangements. Our theoretical investigations suggest that for the photorearrangement of 1,4-dimethyl-imidazole both mechanisms are comparable. On the other hand, for the photorearrangement of 1,4,5-trimethyl-imidazole path 1 should be favored over path 2. Our present theoretical results agree with the available experimental observations.

I. Introduction

Imidazole is the simplest representative of a family of heteroaromatic five-membered compounds containing two nitrogen atoms. It is a building block of several biologically important organic molecules such as nucleotide bases (for example, purines),[1] histidines,[2] and amino acids.[3] Because of its importance, this molecule has been the subject of several investigations. For instance, its molecular geometry was determined by microwave spectroscopy.[3] Also, the infrared spectrum of imidazole was determined in both the gas and liquid phases.[4] Several theoretical calculations have been carried out to obtain its protonation energies in both phases.[5] Since imidazole exerts its biological effects in the gas phase and in aqueous solution, studies of its photochemistry as well as its photophysics are of paramount importance. In 1967, the remarkable photochemical rearrangements of 1,4-dimethyl-imidazole to 1,2-dimethyl-

imidazole and 1,4,5-trimethyl-imidazole to 1,2,5-timethyl-imidazole, as shown in eqs 1 and 2, were first reported by Beak,

Miesel, and Messer.[6,7] Since this discovery, the scope of such photochemical isomerizations to yield new imidazole derivatives has been extended to various photochemical transpositions.[8] In particular, this photochemical rearrangement is important because it represents a key step in one of the pathways proposed for the prebiological synthesis of new species.[9]

---

† E-mail: midesu@mail.ncyu.edu.tw.

As one can see in eqs 1 and 2, these photoreactions involve a formal interchange of the 1,5 or the 2,4 carbons of the imidazole ring. Indeed, permutations of ring atoms are one of the best known features in the photochemical behavior of heterocyclic organic compounds.[10] Several proposals have been considered to describe the intimate mechanism of such reorganizations of the imidazole molecular skeleton.[7,10a] Interested readers can find an excellent review in ref 10a. Beak and Messer, however, performed an extensive study of the photoisomerizations in 2-deuterio-1,4-dimethyl-imidazole.[7] By analyzing the interchange of labeled ([2]D and substituent) ring atoms, they proposed the internal cyclization–isomerization route. Nevertheless, such a study has not yet been confirmed by any kind of theoretical calculation. In fact, as far as we are aware, until now no quantum chemical studies have been performed on imidazole photorearrangements.

It is astonishing that so far there has been only one theoretical investigation concerning the photoisomerization of enaminonitriles to imidazoles,[11] considering the importance of imidazole in biochemistry[1,2] and the extensive research activity on such five-membered species.[12] In order to rationalize the photochemical processes shown in eqs 1 and 2, we thus performed a theoretical investigation of the photorearrangements of 1,4-dimethyl-imidazole (**Rea-1**) and 1,4,5-trimethyl-imidazole (**Rea-2**). In this paper we give a deeper insight into the seemingly complex mechanism of imidazole photorearrangements. Understanding the nature of thermally unstable intermediates and the transition structures of ground states, whose properties may be calculated but not measured because of their short lifetimes, might aid in the understanding of the photochemical rearrangements of imidazoles. Especially, it will be shown below that the conical intersections[13] play a crucial role in the photochemical rearrangements of imidazoles.

In fact, it has been shown recently that conical intersections play a key role in many photochemical reactions.[13] Conical intersections correspond to crossings between states of the same multiplicity (most commonly singlet–singlet). In suitable conditions, they represent very efficient "funnels" for radiationless deactivation or chemical transformation of the system. In this work, the conical intersection regions on the potential surface where decay to the ground-state surface can occur have been located, and ground-state reaction paths leading from these conical intersections to a variety of products have been identified. On the basis of this information, the reaction process is explained. We envision that the present combination of observed experimental work and theoretical examination will provide a comprehensive understanding of the excited-state behavior of imidazoles.

II. Methology

All geometries were fully optimized without imposing any symmetry constraints, although in some instances the resulting structures showed various elements of symmetry. The CASSCF calculations were performed using the multiconfigurational self-consistent field (MCSCF) program released in Gaussian 03.[14]

The active space for describing the photorearrangements of imidazoles comprises 10 electrons in 8 orbitals, i.e., 5 p–π orbitals plus one nonbonding orbital and 2 σ(C–N), σ*(C–N) orbitals. The CASSCF method was used with the 6-311G(d) basis sets for geometry optimization (vide infra). The optimization of conical intersections was achieved in the $(f − 2)$-dimensional intersection space using the method of Bearpark et al.[15] implemented in the Gaussian 03 program. Every stationary point was characterized by its harmonic frequencies

computed analytically at the CASSCF level. Localization of the minima and conical intersection minima was performed in Cartesian coordinates; therefore, the results are independent of any specific choice of internal variables.
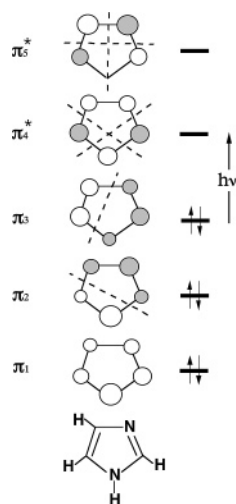
To correct the energetics for dynamic electron correlation, we have used the multireference Møller–Plesset (MP2-CAS) algorithm[16] as implemented in the program package Gaussian 03. Unless otherwise noted, the relative energies given in the text are those determined at the MP2-CAS-(10,8)/6-311G(d) level using the CAS(10,8)/6-311G(d) (hereafter designed MP2-CAS and CASSCF, respectively) geometry.

III. General Consideration

Experimentally, it was reported that the absorption spectra of unsubstituted imidazole in both ethanol and aqueous solutions exhibit two broad bands with maxima around 207 nm (139 kcal/mol) and 187−178 nm (153−161 kcal/mol).[17−24] They are, in general, experimentally and theoretically assigned to the singlet $^1\pi \rightarrow {}^1\pi^*$ transition.[17−24] To the author's knowledge, there has been no reported UV spectrum of imidazole in the gas phase. That is to say, all experimental information on the electronic spectrum of imidazole stems from measurements in liquids. In one elegant theoretical study performed by Serrano-Andrés, Fülscher, Ross, and Merchán,[24] it was suggested that the first and second $\pi \rightarrow \pi^*$ excited singlet valence states of imidazole in the gas phase occur at 155 and 165 kcal/mol, and they shift to 146 and 151 kcal/mol upon solvation. Also, they predicted that the oscillator strengths are 0.036 in ethanol and 0.024 in water for the first valence singlet state but 0.307 in ethanol and 0.275 in water for the second state, the latter being drastically larger than the former. In consequence, the predicted oscillator strengths seem to suggest that the first should be a weak band and the second a strong band. In principle, their computed results are in agreement with the observed absorption band maxima in aqueous solution for imidazole.[17−24] Unfortunately, there are no experimental geometries and spectra for the 1,4-dimethyl-imidazole (**Rea-1**) and 1,4,5-trimethyl-imidazole (**Rea-2**) species studied in the present work as yet available to allow for a definitive comparison. Nevertheless, experimentalists have found no indication of the participation of a triplet state in the photorearrangement of these species.[6,7] That is, the triplet states play no role in the reactions studied in the present work. Because of this, the photochemical rearrangement reactions of these methyl substituted imidazoles should proceed on singlet surfaces and only involve the $\pi \rightarrow \pi^*$ transition. We shall therefore focus on $^1(\pi, \pi^*)$ surfaces from now on.

In order to confirm the accuracy of the theoretical calculations presented in this work, we next consider the Franck−Condon effect, which should play an important role in the photochemical reactions. In the first step, the reactant is excited to its excited singlet state by a vertical excitation. However, as mentioned above, no experimental results, neither gas- nor solution-phase, are available for the vertical transitions of **Rea-1** and **Rea-2** themselves. Nonetheless, our MP2-CAS results estimate that the calculated $^1\pi \rightarrow {}^1\pi^*$ excited-state energy at the Franck−Condon geometry for 1,4-dimethyl-imidazole (**Rea-1**) and 1,4,5-trimethyl-imidazole (**Rea-2**) is 164 (174 nm) and 156 (183 nm) kcal/mol, respectively. These values for **Rea-1** and **Rea-2** agree reasonably with the experimental observations for unsubstituted imidazole as mentioned earlier.[17−24] One should keep in mind that these model reactants contain three methyl substituents, and we feel that the accuracy of the calculations is sufficient for the following investigations of the mechanisms of rearrangements (vide infra).
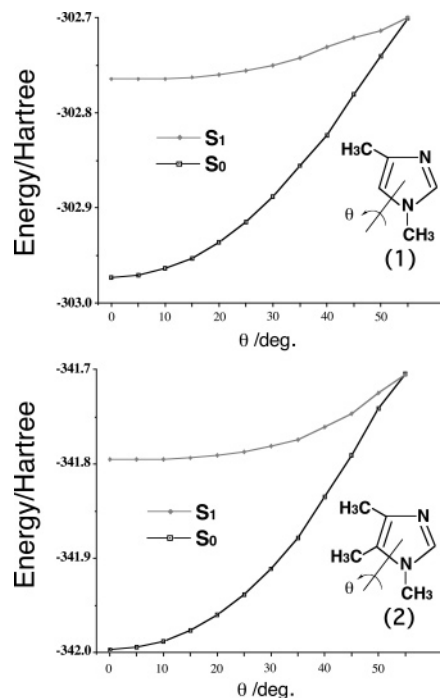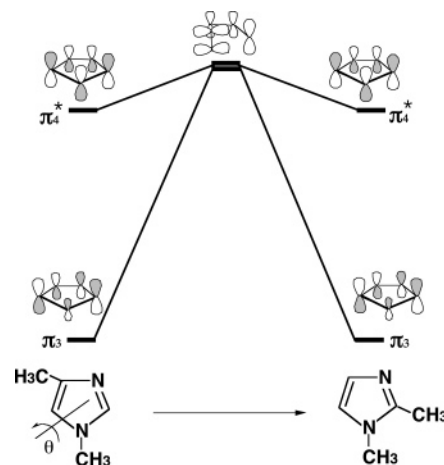
Photochemical Rearrangement Pathways of Imidazoles

J. Phys. Chem. A, Vol. 111, No. 9, 2007 **1569**

SCHEME 1

SCHEME 2

SCHEME 3

A general outline of the five p−π orbitals in unsubstituted imidazole has been given in Scheme 1. As seen in this picture, the lowest singlet $\pi \rightarrow \pi^*$ excitation is the singlet π_3 (HOMO) $\rightarrow \pi_4^*$ (LUMO) transition. It is worth noting that the intermixing of π and π^* levels in imidazole redistributes the electron density. As a result, in the perturbed HOMO level, the electron density (via the atomic orbital coefficients) is increased on the two ortho-carbon atoms with a reduced π electron density on the protonated nitrogen atom. Correspondingly, the coefficients at the protonated nitrogen and the two ortho positions have increased in the perturbed LUMO level. Since the π-electronic structures of methyl substituted imidazoles are similar to those of unsubstituted imidazole, their photoexcitations should be comparable. In fact, methyl substitution in imidazole might change the energy of the excited states slightly owing to methyl hyperconjugation, but the basic photoexcitation features are not expected to change significantly. Again, it is believed that the present models with the current methods (CASSCF and MP2-CAS) employed in this study should provide reliable information for the discussion of the reaction mechanisms.

The central novel feature of the photochemical mechanisms of these methyl substituted imidazoles (**Rea-1** and **Rea-2**) is the location of their conical intersections in the excited- and ground-electronic states. In this work, we shall use the p−π orbital model as outlined in Scheme 1 to search for the conical intersections of the photorearrangements of the **Rea-1** and **Rea-2** molecules, which are π valence isoelectronic to benzene. Scheme 2 shows the qualitative potential energy curves for the S_0 and S_1 states of **Rea-1** and **Rea-2** as a function of rotation about the $C_5=N_1$ (N_1 is the methyl substituted nitrogen atom) double bond (i.e., the rotation angle θ).[25] When the $C_5=N_1$ π bonds in **Rea-1** and **Rea-2** are twisted, both p_3 and π_4^* are raised in energy because of increased antibonding interactions. In consequence, these π orbitals become degenerate at a geometry around 55° rotation for **Rea-1** and **Rea-2** as shown in Scheme 2. In other words, this excitation removes the barrier to rotation about the former $C_5=N_1$ axis, and rotation toward an out-of-plane orientation of the p−π orbitals lowers the energy of the excited state. See Scheme 3. Although these out-of-plane angles were obtained without full optimization of the reactants, they at least gave us a hint that a degeneracy between the HOMO and the LUMO can exist after the rotation of one $C_5=$ N_1 bond. Furthermore, the formation of such a degenerate point provides further evidence for an enhanced intramolecular rotation in the five-membered ring geometry and possibly the existence of a conical intersection, where decay to the ground

state can be fully efficient. It should be pointed out that the return to S_0 through a conical intersection at such a distorted quasi-tetrahedral geometry is basically similar to both the H_4[26a] and the pericyclic[26b,c] models proposed previously. In any event, we shall utilize the above result to interpret the mechanisms for the photochemical rearrangement reactions of **Rea-1** and **Rea-2** in the following section.

IV. Results and Discussion

(1) 1,4-Dimethyl-imidazole. We first consider the photoisomerization of 1,4-dimethyl-imidazole (**Rea-1**) as indicated in eq 1. As pointed out previously, there could be two kinds of reaction pathways for the imidazole photorearrangement reaction, i.e., a conical intersection pathway (path 1) and an internal cyclization−isomerization pathway (path 2), which all lead to the same photoproduct, 1,2-dimethyl-imidazole (**Pro-1**). Figure 1 contains the relative energies of the various points with respect to the energy of the reactant, 1,4-dimethyl-imidazole (**Rea-1**). Also, these relative energies obtained using both CASSCF and MP2-CAS methods are presented in Table 1. The structures of

1570 *J. Phys. Chem. A, Vol. 111, No. 9, 2007*

Su

TABLE 1: Energies (in kcal/mol) of the Critical Points Located along the Paths 1 and 2 at the CAS(10,8)/6-311G(d) and MP2-CAS(10,8)/6-311G(d)//CAS(10,8)/6-311G(d) (in Parentheses) Levels of Theory (See Figures 1 and 2)

structure	state	$\Delta E_{rel}{}^a$
1,4-dimethyl-imidazole (**1**)	S_0	0.0 (0.0)
FC-A	S_1	162.1 (164.2)
CI-1	S_1/S_0	111.0 (108.6)
CI-2	S_1/S_0	109.5 (110.6)
3	S_0	67.09 (54.25)
TS-1	S_0	105.0 (88.12)
4	S_0	70.33 (66.56)
TS-2	S_0	103.1 (85.69)
1,2-dimethyl-imidazole (**Pro-1**)	S_0	−10.71 (−6.683)

*^{a} Energy relative to 1,4-dimethyl-imidazole (**1**).*

the various critical points on the possible mechanistic pathways of Figure 1 are demonstrated in Figure 2. Cartesian coordinates and energetics calculated for the various points with both methods are available as Supporting Information.

In the first step, the reactant (1,4-dimethyl-imidazole, **Rea-1**) is excited to its excited singlet state by a vertical excitation as shown in the middle of Figure 1. After the vertical excitation process, the molecule is situated on the excited singlet surface but still possesses the S_0 (ground-state) geometry. As mentioned previously, the vertical excitation energy (**FC-A**) for **Rea-1** was calculated to be 162 and 164 kcal/mol for CASSCF and MP2-CAS levels of theory, respectively. No experimental data are presently available for its vertical excitation energy. Nevertheless, as stated earlier, comparison with the spectra of unsubstituted imidazole[17−24] leads us to believe that the calculated vertical excitation energy for **FC-A** presented here should be reliable for further discussion.

On the basis of the earlier prediction, we searched for a conical crossing point between the S_0 and S_1 surfaces for path

1. As already shown in Scheme 2, since the formation of a narrow energy gap between the S_0 and S_1 states can occur by twisting one $C_5{=}N_1$ double bond, this strongly implies the existence of a conical intersection at a nearby geometry. Thus, we fully optimized the nonplanar geometry by twisting structure **Rea-1**. As a result, the lowest energy point of the intersection seam of the S_0 and S_1 states was located for path 1, which was identified as **CI-1** as presented in Figures 1 and 2. A plot of the surface energies in the immediate vicinity of the crossing point has the form of a double cone,[13] which is shown in Scheme 4. The directions of the derivative coupling and gradient difference vectors, which are also plotted in Figure 2, define a plane in the space of nuclear motions. Motion in this plane (the branching space) lifts the degeneracy, while the energy has been minimized in the remaining $(n − 2)$-dimensional space.[13] That is to say, funneling through the S_1/S_0 **CI-1** conical intersection can lead to two different reaction pathways on the ground state surface via either the derivative coupling vector or the gradient difference vector.[13] The derivative coupling vector for **CI-1** corresponds to an antisymmetric bending motion, which leads to a vibrationally hot species at the S_0 configuration. On the other hand, its gradient difference vector corresponds to the intramolecular rotation via the $C_5{=}N_1$ double bond. Indeed, following the gradient difference vector from **CI-1** and rotating the $C_5{=}N_1$ bond result in swapping the two neighboring ring atoms (N_1 and C_5), i.e., 1,4-dimethyl-imidazole (**Pro-1**). In consequence, the S_1/S_0 **CI-1** conical intersection corresponds
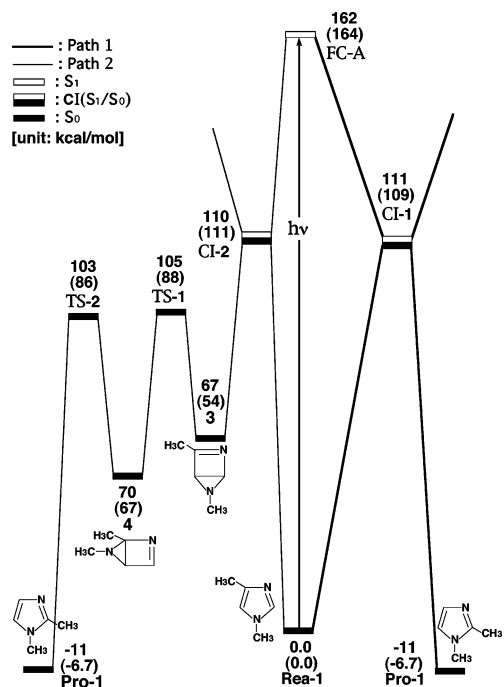

Figure 1. Energy profiles for the photoisomerization modes of 1,4-dimethyl-imidazole (**Rea-1**). The abbreviations FC and CI stand for Franck−Condon and conical intersection, respectively. The relative energies were obtained at the MP2-CAS-(10,8)/6-311G(d)//CAS(10,8)/6-311G(d) and CAS(10,8)/6-311G(d) (in parentheses) levels of theory. All energies (in kcal/mol) are given with respect to the reactant (**Rea-1**). See Figure 2 for the CASSCF optimized structures of the crucial points. For more information see the text.
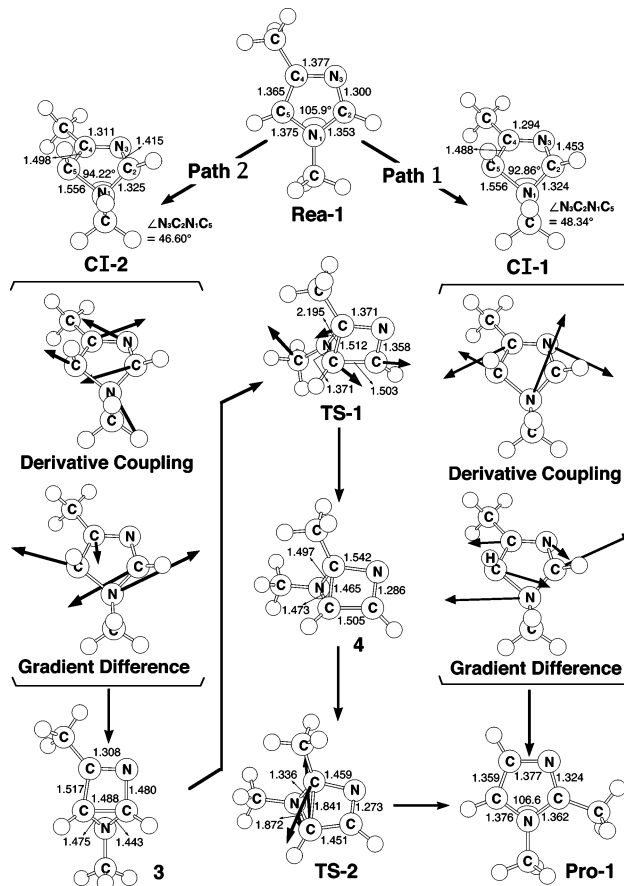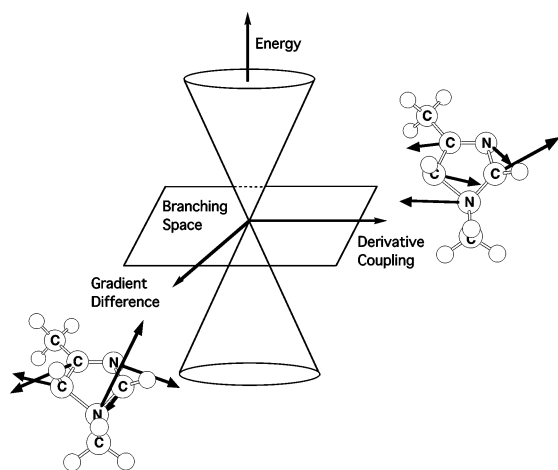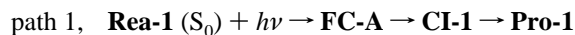

Figure 2. The CAS(10,8)/6-311G(d) geometries (in Å and deg) for path 1 and path 2 of 1,4-dimethyl-imidazole (**Rea-1**), conical intersection (CI), intermediate, transition state (TS), and isomer products. The derivative coupling and gradient difference vectors, −those which lift the degeneracy,− were computed with CASSCF at the conical intersections **CI-1** and **CI-2**. The corresponding CASSCF vectors are shown in the inset. For more information see the Supporting Information.

Photochemical Rearrangement Pathways of Imidazoles

J. Phys. Chem. A, Vol. 111, No. 9, 2007 **1571**

SCHEME 4

to the global minimum of the 1,2-dimethyl-imidazole/1,4-dimethyl-imidazole π/π^* excited-state surface. It should be emphasized here that although the energy is minimized, the structure **CI-1** shown in Figures 1 and 2 and Scheme 4 is just a conical intersection rather than a true minimum[13] because its energy gradient does not go to zero.
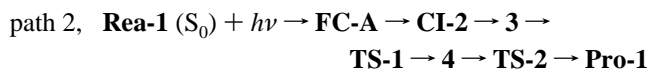
Our CASSCF calculations reveal that the planarity of **CI-1** is lost and the dihedral angle $\angle N_3C_2N_1C_5$ is 46.60° as illustrated in Figure 2. Additionally, our MP2-CAS computational results indicate that the energy of **CI-1** relative to the ground state minimum (**1**) is 109 kcal/mol but lower than the **FC-A** by 56 kcal/mol in energy. Accordingly, our computations predict that the photochemical rearrangement reaction of path 1 should be a barrierless process. That is, starting from the **FC-A** point, 1,4-dimethyl-imidazole (**Rea-1**) enters an efficient decay channel, **CI-1**. After decay at this conical intersection point, the observed photoproduct (**Pro-1**) as well as reactant (**Rea-1**) can be reached via a barrierless ground-state relaxation pathway. Thus, our theoretical calculations demonstrate that photoreaction path 1 of reactant **Rea-1** can be represented as follows:

path 1, **Rea-1** $(S_0) + h\nu \rightarrow$ **FC-A** $\rightarrow$ **CI-1** $\rightarrow$ **Pro-1**

In path 2 (internal cyclization—isomerization path), geometry optimization on the S_1 excited state was performed by valence isomerization with the formation of one chemical bond between C_2 and C_5. The relaxation reaches an S_1/S_0 **CI-2** where the photoexcited system decays nonradiatively to the ground state (S_0). As seen in Figure 2, one C_2-C_5 bond length is shortened to 2.116 Å and the $C_2N_1C_5$ bond angle is also narrowed to 92.86°, compared with their corresponding values in the reactant (**Rea-1**), 2.178 Å and 105.9°, respectively. As a result, from the structure at the S_1/S_0 **CI-2**, the nature of the path 2 potential energy surface can be regarded as C_2-C_5 bond closure, as expected previously. Again, funneling through the conical intersection, different reaction pathways on the ground-state surface may be predicted by following the derivative coupling vector or the gradient difference vector direction as demonstrated in Scheme 4.[13] Examination of these two vectors in **CI-2** provides important information concerning the photorearrangement process of **Rea-1**: the derivative coupling vector gives the asymmetric N_3-C_4 bending motion that leads to a vibrationally hot **Rea-1**-S_0 species, whereas the gradient difference vector is mainly related to the $C_5N_1C_2$ bending mode that gives the bicyclic intermediate (**3**) on the S_0 surface. Namely, intermediate **3** arises from a singlet excited-state 1,3-closure of the $C_5N_1C_2$ atoms. The calculated geometry of **3** is shown in

Figure 2. Here, there exists a nonplanar bicyclic structure with a substituted nitrogen atom (N_1) out of plane by 70.38°. Moreover, our MP2-CAS results estimate that the energy of **3** lies below that of **FC-A** by about 110 kcal/mol. This finding implies that the large excess energy of 110 kcal/mol resulting from the relaxation from **FC-A** to **3** is the driving force for further isomerization reactions on the ground state surface (vide infra).

From the local minimum **3**, a transition state search for the substituted nitrogen (N_1) migration based on the model of the **Rea-1** conformation was undertaken. The optimized transition state structure (**TS-1**) along with the calculated transition vector at the CASSCF level is shown in Figure 2. The arrows indicate the direction in which the substituted N_1 atom moves in the normal coordinate corresponding to the imaginary frequency (202i cm^{-1}). That is, the vibrational motion for the intramolecular migration of a substituted N_1 atom into the C_4-C_5 bond involves the formation of another bicyclic intermediate (**4**). Again, from **4** the isomerization can take place in one direction, in which the C_4-C_5 chemical bond is broken (**TS-2**) to form the five-membered ring species, i.e., the observed photoproduct (**Pro-1**). As a result, our theoretical investigations suggest that the reaction mechanism for path 2 should proceed as follows:

path 2, **Rea-1** $(S_0) + h\nu \rightarrow$ **FC-A** $\rightarrow$ **CI-2** $\rightarrow$ **3** $\rightarrow$
$$\text{**TS-1**} \rightarrow \text{**4**} \rightarrow \text{**TS-2**} \rightarrow \text{**Pro-1**}$$

From these two local minima (**3** and **4**), both isomerizations possess barrier heights, computed to be about 34 kcal/mol for **3** $\rightarrow$ **TS-1** and 24 kcal/mol for **4** $\rightarrow$ **TS-2**. Due to the large excess energy of 110 kcal/mol obtained from the decay of **FC-A** to **3**, both barriers can easily be surmounted. It is noted that photoproduct **Pro-1** is thermodynamically stable, by 6.7 kcal/mol, with respect to reactant **Rea-1**. Furthermore, from the computational data shown in Figure 1, one can readily see that path 1 should be more favorable than path 2 from a kinetic viewpoint. The reason for this is that the former mechanism is a one-step process, while the latter mechanism is a multistep process. Nevertheless, it should be pointed out that **CI-1** and **CI-2** are predicted to be nearly thermoneutral, the former being slightly lower in energy than the latter only by about 2.0 kcal/mol. Owing to such a small energy difference between these two reaction paths, our theoretical findings suggest that path 1 and path 2 should compete with each other during the photochemical reaction of **Rea-1**. As a result, it would take a long time for the photorearrangement of **Rea-1** to occur on path 2, since it would take multiple steps to obtain the final photoproduct. The further supporting experimental evidence comes from the fact that irradiation of **Rea-1** in *tert*-butyl alcohol for 41 h with a high-pressure mercury resonance lamp gives **Pro-1** in 40% conversion (25% yield).[7]

(2) 1,4,5-Trimethyl-imidazole. For comparison, we next consider the photorearrangement of 1,4,5-trimethyl-imidazole **Rea-2** (eq 2). Like the previous study, in this section we shall examine the photochemical reaction pathways corresponding to (i) a conical intersection pathway (path 3) and (ii) an internal cyclization—isomerization pathway (path 4). A schematic overview of the computed energy profile for the photoreaction pathways of **Rea-2** is shown in Figure 3. The structures optimized at the CASSCF and MP2-CAS levels of theory are outlined in Figure 4, with the corresponding energies in Table 2. Cartesian coordinates and energetics calculated for the critical points at these levels are available as Supporting Information.

Figure 3 is arranged as Figure 1, with its center indicating reactant **Rea-2** (S_0) and the point on the singlet excited surface
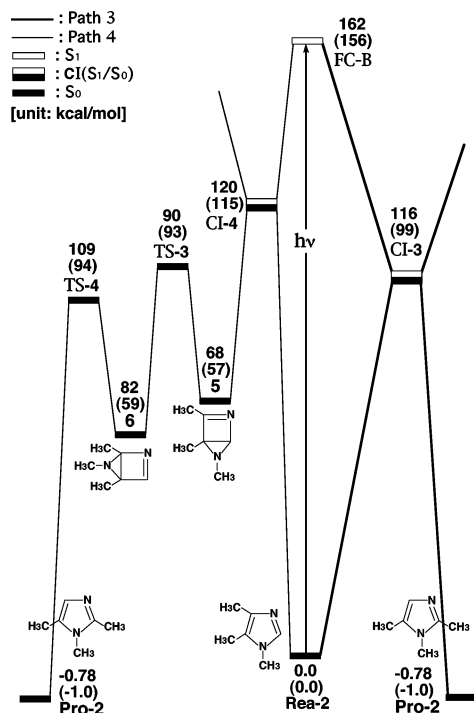
Figure 3. Energy profiles for the photoisomerization modes of 1,4,5-trimethyl-imidazole (**Rea**-**2**). The abbreviations FC and CI stand for Franck−Condon and conical intersection, respectively. The relative energies were obtained at the MP2-CAS-(10,8)/6-311G(d)//CAS(10,8)/6-311G(d) and CAS(10,8)/6-311G(d) (in parentheses) levels of theory. All energies (in kcal/mol) are given with respect to the reactant (**Rea**-**2**). See Figure 4 for the CASSCF optimized structures of the crucial points. For more information see the text.

reached by a vertical excitation **FC-B** (S_1 (S_0 geometry)). The reaction profiles of the conical intersection (path 3) and of the internal cyclization−isomerization (path 4) reaction routes are depicted to the right- and left-hand side of Figure 3, respectively. As mentioned before, the calculated singlet vertical excitation energy (**2** → **FC-B**) is predicted to be about 162 and 156 kcal/mol with respect to the corresponding reactant **2**, for CASSCF and MP2-CAS levels of theory, respectively. To our knowledge, no experimental data concerning the vertical excitation energy are available in the literature. Nevertheless, comparison with the vertical excitation energy of unsubstituted imidazole, as given in the previous section, suggests that the methyl substituents on such five-membered systems do not significantly affect the first singlet excitation energy.

The geometry optimization starting from **FC-B** leads to the conical intersections (**CI-3** and **CI-4**), which belong to two kinds of reaction pathways, i.e., path 3 and path 4, respectively. As in the case of Scheme 4, their derivative coupling and gradient difference vectors obtained at the conical intersections are given in Figure 4. These conical intersections can efficiently funnel molecules from the $^1(\pi\pi^*)$-state to the ground-state surface. Also, these funnels, which are easily accessed once the $^1(\pi\pi^*)$ surface is populated, determine the reaction path taken on the ground-state surface.[13]

In path 3, as in the case of path 1 in **1**, geometry optimization on the S_1 $^1(\pi \rightarrow \pi^*)$ excited state was performed by rotating the N_1=C_5 double bond of **2**. The relaxation reaches S_1/S_0 **CI-3** where the photoexcited system decays nonradiatively to S_0. As seen in Figure 4, our CASSCF results demonstrate that the planarity of **CI-3** is lost and its optimized dihedral angle $\angle N_1 C_2 N_3 C_4$ is 50.69°. As discussed before, according to the results outlined in Figure 4, funneling through S_1/S_0 **CI-3** leads
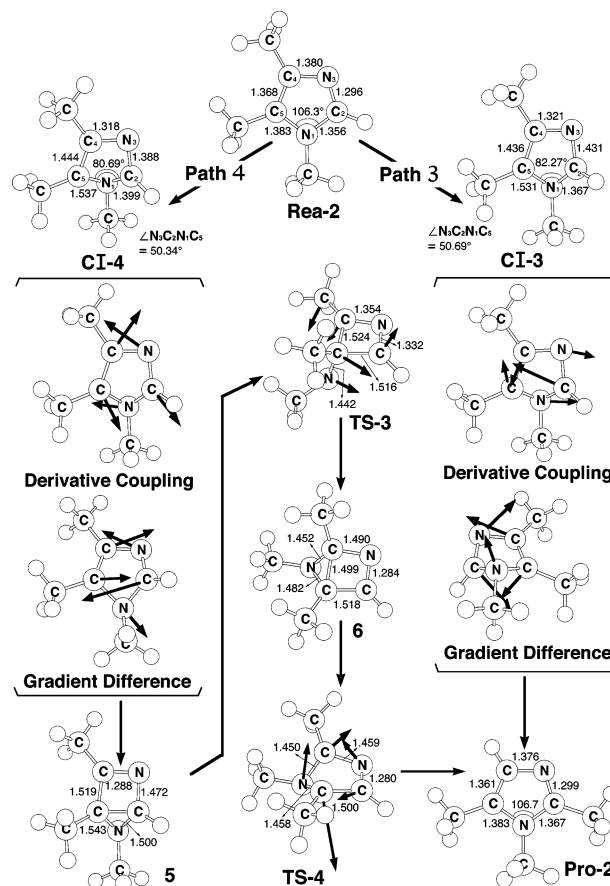

Figure 4. The CAS(10,8)/6-311G(d) geometries (in Å and deg) for path 3 and path 4 of 1,4,5-trimethyl-imidazole (**Rea**-**2**), conical intersection (**CI**), intermediate, transition state (**TS**), and isomer products. The derivative coupling and gradient difference vectors, − those which lift the degeneracy,− were computed with CASSCF at the conical intersections **CI-3**. The corresponding CASSCF vectors are shown in the inset. For more information see the Supporting Information.
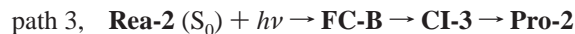
TABLE 2: Energies (in kcal/mol) of the Critical Points Located along the Paths 3 and 4 at the CAS(10,8)/6-311G(d) and MP2-CAS(10,8)/6-311G(d)//CAS(10,8)/6-311G(d) (in Parentheses) Levels of Theory (See Figures 3 and 4)

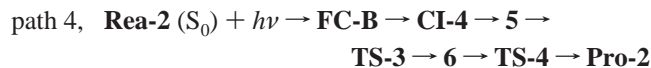| structure	state	$\Delta E_{rel}{}^a$
1,4,5-trimethyl-imidazole (**2**)	S_0	0.0 (0.0)
FC-B	S_1	162.0 (156.6)
CI-3	S_1/S_0	116.2 (98.85)
CI-4	S_1/S_0	120.2 (114.7)
5	S_0	67.64 (56.86)
TS-3	S_0	90.32 (93.36)
6	S_0	81.78 (58.82)
TS-4	S_0	108.7 (93.90)
1,2,5-trimethyl-imidazole (**Pro**-**2**)	S_0	−0.7781 (−1.004)

^{a} Energy relative to 1,4,5-trimethyl-imidazole (**2**).

to two different reaction paths on the ground-state surface, via either the derivative coupling vector or the gradient difference vector.[13] The derivative coupling vector for **CI-3** corresponds to an antisymmetric C_2=C_5 bending motion, which leads to a vibrationally hot species at the S_0 geometry. On the other hand, its gradient difference vector corresponds to the intramolecular rotation of an N_1=C_5 double bond. Indeed, following the gradient difference vector from **CI-3**, the system arrives at a new five-membered photoproduct, 1,2,5-trimethyl-imidazole (**Pro**-**2**). As can be seen in Figure 3 and Table 2, our MP2-

Photochemical Rearrangement Pathways of Imidazoles

J. Phys. Chem. A, Vol. 111, No. 9, 2007 **1573**

CAS results suggest that **CI-3** is 57 kcal/mol lower in energy than **FC-B** but 99 kcal/mol higher in energy than its corresponding reactant **Rea-2**. Accordingly, our theoretical investigations indicate that path 3 can proceed as follows:

$$\text{path 3,} \quad \textbf{Rea-2}\ (S_0) + h\nu \rightarrow \textbf{FC-B} \rightarrow \textbf{CI-3} \rightarrow \textbf{Pro-2}$$

In path 4, the system relaxes from the **FC-B** point to the conical intersection (**IC-4**), the latter being lower in energy than the former by 41 kcal/mol. Its key structural parameters are given in Figure 4, accompanied by the derivative coupling vector and the gradient difference vector. By analogy with the case of **CI-2**, the CASSCF results indicate that **CI-4** has a significantly narrower bond angle ($\angle C_2N_1C_5 = 50.34°$) and a shorter bond distance (i.e., $C_2-C_5 = 1.900$ Å) than its corresponding **Rea-2** ($\angle C_2N_1C_5 = 106.3°$ and $C_2-C_5 = 2.192$ Å). On the basis of the results given in Figure 4, funneling through S_1/S_0 **CI-4** leads to two different reaction paths on the ground-state surface, via either the derivative coupling vector or the gradient difference vector. On one hand, the derivative coupling vector for **CI-4** corresponds to the N_1-C_5 and N_3-C_4 stretching motions, which lead to vibrationally hot species at the S_0 configuration. On the other hand, the gradient difference vector corresponds to the intramolecular formation of a bicyclic species (**5**). This local intermediate is nonplanar with the substituted nitrogen atom (N_1) out of plane by 72.10°. Then, a [1,3] sigmatropic shift of the N_1 atom must take place via a transition state (**TS-3**) to give another local intermediate **6**. Again, this species has a nonplanar conformation with the N_1 atom out of plane by 60.74°. This then undergoes a ring opening via a transition state (**TS-4**) to form the observed photoproduct (**Pro-2**). Namely, our computational results suggest that the mechanism for path 4 should be represented as follows:

$$\text{path 4,} \quad \textbf{Rea-2}\ (S_0) + h\nu \rightarrow \textbf{FC-B} \rightarrow \textbf{CI-4} \rightarrow \textbf{5} \rightarrow$$
$$\textbf{TS-3} \rightarrow \textbf{6} \rightarrow \textbf{TS-4} \rightarrow \textbf{Pro-2}$$

Our MP2-CAS results indicate that the relative energies of these critical points are 156, 115, 57, 93, 59, 94, and −1.0 kcal/mol for **FC-B**, **CI-4**, **5**, **TS-3**, **6**, **TS-4**, and **Pro-2**, respectively, with respect to the corresponding ground-state reactant **Rea-2**. It is worth noting that **FC-B** lies 99 kcal/mol above **5**. Namely, 1,4,5-trimethyl-imidazole (**Rea-2**) possesses an excess energy of about 99 kcal/mol arising from the relaxation to the local minimum **5**. Our computational results also indicate that the barrier heights from **5** to **TS-3** and from **6** to **TS-4** are 36 and 35 kcal/mol, respectively. As a consequence, because of such a large excess energy (99 kcal/mol) obtained from the decay of **FC-B** to **5**, both barriers can readily be surmounted. Nevertheless, our present MP2-CAS results demonstrate that **CI-3** is lower in energy than **CI-4** by 16 kcal/mol. The model calculations thus predict that path 3 should be favored over path 4 from a kinetic viewpoint. Indeed, it was reported that photolysis of **Rea-2** in ethanol with a low-pressure mercury lamp gives approximately 40% **Pro-2**,[6,7] its yield being much larger than that in the case of **Rea-1** with the same conditions. Consequently, our theoretical predictions presented in this work are in good agreement with the experimental observations.

V. Conclusion

The photochemical reaction pathways of 1,4-dimethyl-imidazole (**Rea-1**) and 1,4,5-trimethyl-imidazole (**Rea-2**) were investigated by ab initio calculations at CAS(8,7)/6-311G(d) and MP2-CAS-(8,7)/6-311G(d)//CAS(8,7)/6-311G(d) levels of theory. In the present work, two reaction pathways, the conical

intersection route (path 1 and path 3) and the internal cyclization—isomerization route (path 2 and path 4), were also examined theoretically. Our results demonstrate that the photorearrangements of such five-membered species are similar to each other. In the conical intersection route (path 1), both reactants are initially excited to the first singlet excited state ($^1\pi \rightarrow ^1\pi^*$). Then, photochemically active relaxation from the $S_1(^1\pi^*)$ to the ground state leads to an S_1/S_0 conical intersection where the photoexcited system decays nonradiatively to the ground state (S_0). Relaxation on the S_1 surface causes the intramolecular exchange between two neighboring atoms, from which one may obtain the observed photoproduct. On the other hand, in the internal cyclization—isomerization route (path 2), the pathway consists of a sequence of small geometric rearrangements, which may lead to either the final photoproduct or a return to the reactant.

Our theoretical investigations suggest that for 1,4-dimethyl-imidazole (**Rea-1**) these two reaction pathways should compete with each other, since the energetics for both conical interaction points (**CI-1** and **CI-2**) are quite similar to each other. It should be noted that the former mechanism is a one-step process, while the latter is a multistep process. Therefore we expect a low overall quantum yield for the rearrangement, as the involvement of **CI-2** leads to slow rearrangement via multiple activated steps. For the 1,4,5-trimethyl-imidazole (**Rea-2**) molecule, however, our theoretical study suggests that the single step path 3 (the conical intersection route) should be favored over the multistep path 4 (the internal cyclization—isomerization route). The reason for that is because the energy of the conical intersection (**CI-3**) for the former mechanism is lower than that (**CI-4**) for the latter by a calculated 16 kcal/mol. As a result, we predict that the quantum yield for **Rea-2** will be larger than that of **Rea-1**, which is in accordance with the experimental observations.[6,7]

It is hoped that the present work can stimulate further research into this subject.

References and Notes

(1) (a) Cooper, D. G.; Young, R. C.; Durant, G. J.; Ganellin, C. R. *Comprehensive Medicinal Chemistry*; Pergamon Press, 1990; Vol. 3, pp 323−421. (b) Gupta, R. R.; Kumar, M.; Gupta, V. *Heterocyclic Chemistry*; Springer: Berlin, 1998; Vols. 1 and 2.

(2) (a) Ochiai, E.-I. In *Bioinorganic Chemistry: An Introduction*; Busch, D. H., Shull, H., Eds.; Allyn and Bacon: Boston, 1977. (b) Creighton, T. E. *Proteins, Structures and Molecular Principles*; Freeman, W. H. and Co.: New York, 1983. (b) Kang, P.; Foote, C. S. *J. Am. Chem. Soc.* **2002**, *124*, 9629.

(3) Christen, D.; Griffiths, J. H.; Sheridan, J. *Z. Naturforsch., A* **1981**, *36*, 1378.

(4) (a) Bellocq, A. M.; Perchard, C.; Novark, A.; Josien, M. L. *J. Chim. Phys. Phys.-Chim. Biol.* **1965**, *62*, 1334. (b) Perchard, C.; Bellocq, A. M.; Novark, A. *J. Chim. Phys. Phys.-Chim. Biol.* **1965**, *62*, 1344. (c) King, S.

T. *J. Phys. Chem.* **1970**, *74*, 2133. (d) Markham, L. M.; Mayne, L. C.; Hudson, B. S.; Zgierski, M. Z. *J. Phys. Chem.* **1993**, *97*, 10319.

(5) (a) Mo, O.; de Paz, J. L. G.; Yanez, M. *J. Phys. Chem.* **1986**, *90*, 5597. (b) Lim, C.; Bashford, D.; Karplus, M. *J. Phys. Chem.* **1991**, *95*, 5610. (c) Nagy, P. I.; Durant, G. J.; Smith, D. A. Unpublished results.

(6) Beak, P.; Miesel, J. L.; Messer, W. R. *Tetrahedron Lett.* **1967**, 5315.

(7) Beak, P.; Messer, W. *Tetrahedron* **1969**, *25*, 3287.

(8) (a) Buchardt, O. In *Photochemistry of Heterocyclic Compounds*; Wiley: New York, 1976. (b) Kopecky, J. In *Organic Photochemistry: A Visual Approach*; VCH Publishers: New York, 1992.

(9) (a) Pavlik, J. W.; Tongcharoensirikul, P.; Bird, N. P.; Day, A. C.; Barltrop, J. A. *J. Am. Chem. Soc.* **1994**, *116*, 2292. (b) Su, M.-D. *J. Phys. Chem. A.*, in press.

(10) (a) Padwa, A. In *Rearrangements in Ground and Excited States*; de Mayo, P., Ed.; Academic Press: New York, 1980; Vol. 3, p 501 ff. (b) La-balche-Combier, A. In *Photochemistry of Heterocyclic Compounds*; Burchart, O., Ed.; Wiley-Interscience: New York, 1976; Vol. 4, p 123 ff.

(11) Bigot, B.; Roux, D. *J. Org. Chem.* **1981**, *46*, 2872.

(12) (a) Ferris, J. P.; Trimmer, R. W. *J. Org. Chem.* **1976**, *41*, 19. (b) Goff, H. *J. Am. Chem. Soc.* **1980**, *102*, 3252. (b) Bolton, J. L.; McClelland, R. A. *J. Am. Chem. Soc.* **1989**, *111*, 8172. (c) Kang, P.; Foote, C. S. *J. Am. Chem. Soc.* **2002**, *124*, 9629.

(13) (a) Bernardi, F.; Olivucci, M.; Robb, M. A. *Isr. J. Chem.* **1993**, 265. (b) Klessinger, M. *Angew. Chem., Int. Ed. Engl.* **1995**, *34*, 549. (c) Bernardi, F.; Olivucci, M.; Robb, M. A. *Chem. Soc. Rev.* **1996**, 321. (d) Bernardi, F.; Olivucci, M.; Robb, M. A. *J. Photochem. Photobiol., A* **1997**, *105*, 365. (e) Klessinger, M. *Pure Appl. Chem.* **1997**, *69*, 773. (f) Domcke, W., Yarkony, D. R., Koppel, H., Eds. *Conical Intersections: Electronic Structure, Dynamics and Spectroscopy*; Advanced Series in Physical Chemistry-Vol. 15; Imperial College Press: London, 2006.

(14) Frisch, M. J.; Trucks, G. W.; Schlegel, H. B.; Scuseria, G. E.; Robb, M. A.; Cheeseman, J. R.; Zakrzewski, V. G.; Montgomery, J. A., Jr.; Stratmann, R. E.; Burant, J. C.; Dapprich, S.; Millam, J. M.; Daniels, A. D.; Kudin, K. N.; Strain, M. C.; Farkas, O.; Tomasi, J.; Barone, V.; Cossi, M.; Cammi, R.; Mennucci, B.; Pomelli, C.; Adamo, C.; Clifford, S.; Ochterski, J.; Petersson, G. A.; Ayala, P. Y.; Cui, Q.; Morokuma, K.; Malick, D. K.; Rabuck, A. D.; Raghavachari, K.; Foresman, J. B.; Cioslowski, J.; Ortiz, J. V.; Baboul, A. G.; Stefanov, B. B.; Liu, G.; Liashenko, A.; Piskorz, P.; Komaromi, I.; Gomperts, R.; Martin, R. L.; Fox, D. J.; Keith, T.; Al-Laham, M. A.; Peng, C. Y.; Nanayakkara, A.; Gonzalez, C.; Challacombe, M.; Gill, P. M. W.; Johnson, B.; Chen, W.; Wong, M. W.; Andres, J. L.; Gonzalez, C.; Head-Gordon, M.; Replogle, E. S.; Pople, J. A. *Gaussian 03*; Gaussian, Inc.: Pittsburgh, PA, 2003.

(15) Bearpark, M. J.; Robb, M. A.; Schlegel, H. B. *Chem. Phys. Lett.* **1994**, *223*, 269.

(16) McDouall, J. J. W.; Peasley, K.; Robb, M. A. *Chem. Phys. Lett.* **1988**, *148*, 183.

(17) Fawcett, T. G.; Bernarducci, E. R.; Krogh-Jespersen, K.; Schurgar, H. J. *J. Am. Chem. Soc.* **1980**, *102*, 2598.

(18) Bernarducci, E. R.; Bharadwaj, P. K.; Krogh-Jespersen, K.; Potenza, J. A.; Schurgar, H. J. *J. Am. Chem. Soc.* **1983**, *105*, 3860.

(19) Caswell, D. S.; Spiro, T. G. *J. Am. Chem. Soc.* **1986**, *108*, 6470.

(20) Leandri, G.; Mangini, X.; Montanari, F.; Passerini, R. *Gazz. Chim. Ital.* **1955**, *85*, 769.

(21) Gelus, M.; Bonnier, J. *J. Chim. Phys. Phys.-Chim. Biol.* **1967**, *64*, 1602.

(22) Grebow, P. E.; Hooker, T. M. *Biopolymers* **1975**, *14*, 871.

(23) Asher, S. A.; Murtaugh, T. L. *Appl. Spectrosc.* **1988**, *42*, 83.

(24) Serrano-Andrés, L.; Fülscher, M. P.; Ross, B. O.; Merchán, M. *J. Phys. Chem.* **1996**, *100*, 6484.

(25) The C−C, C−N, C−H, N−CH$_3$, and C−H$_3$ bonds in **1** and **2** are fixed to be 1.44, 1.35, 1.09, 1.39, and 1.45 Å, respectively. Also, the ∠NCC, ∠CNC, ∠NCN, ∠HCN, ∠HCH, and ∠CCC bond angles are fixed to be 106°, 106°, 110°, 120°, 109°, and 120°, respectively.

(26) (a) Gerhartz, W.; Poshusta, R. D.; Michl, J. *J. Am. Chem. Soc.* **1977**, *99*, 4263. (b) Olivucci, M.; Ragazos, I. N.; Bernardi, F.; Robb, M. A. *J. Am. Chem. Soc.* **1993**, *115*, 3710. (c) Olivucci, M.; Bernardi, F.; Celani, P.; Ragazos, I. N.; Robb, M. A. *J. Am. Chem. Soc.* **1994**, *116*, 1077.